Neuroscience 183 (2011) 178–188

COLLAGEN VI PROTECTS AGAINST NEURONAL APOPTOSIS ELICITED BY ULTRAVIOLET IRRADIATION VIA AN AKT/PHOSPHATIDYLINOSITOL 3-KINASE SIGNALING PATHWAY

I. H. CHENG,[a*] Y.-C. LIN,[a] E. HWANG,[b,c] H.-T. HUANG,[a] W.-H. CHANG,[a] Y.-L. LIU[a] AND C.-Y. CHAO[c,d]

[a]*Institute of Brain Science, National Yang-Ming University, Taipei, Taiwan 11221*

[b]*Institute of Bioinformatics and Systems Biology, National Chiao Tung University, Hsinchu, Taiwan 30068*

[c]*Department of Biological Science and Technology, National Chiao Tung University, Hsinchu, Taiwan 30068*

[d]*Institute of Molecular Medicine and Bioengineering, National Chiao Tung University, Hsinchu, Taiwan 30068*

Abstract—Collagen VI, one of the extracellular matrix proteins, has been implicated in regulating cell proliferation and reducing apoptosis in several different systems. However, the role of collagen VI in the central nervous system remains unclear. In this manuscript, we demonstrated that upon ultraviolet (UV) irradiation, mouse primary hippocampal neurons specifically up-regulate the expression of *Col6a1, Col6a2*, and *Col6a3* mRNA and secreted collagen VI protein. Augmentation of collagen VI mRNA and protein after UV irradiation may have a neuroprotective role as suggested by the fact that extracellular supplying soluble collagen VI protein, but not other collagen proteins, reduced UV induced DNA damage, mitochondria dysfunction, and neurite shrinkage. We also tried to determine the signaling molecules that mediate the protective effect of collagen VI via Western blot and inhibitor analysis. After collagen VI treatment, UV irradiated neurons increased phosphorylation of Akt and decreased phosphorylation of JNK. Inhibiting Akt/Phosphatidylinositol 3-kinases (PI3K) pathway diminished the protective effect of collagen VI. Our study suggested a potential protective mechanism by which neurons up-regulate collagen VI production under stress conditions to activate Akt/PI3K anti-apoptotic signaling pathway.

Key words: collagen VI, neuroprotection, UV, Akt/PI3K, NeurotoxQ.

Appearance of the proper type of extracellular matrix (ECM) proteins not only supports tissue structure, but also plays essential roles in the proliferation, differentiation, and survival for most types of cells (Sherman-Baust et al., 2003; Nelson and Bissell, 2006; Cheresh and Stupack, 2008). In the central nervous system, the ECM proteins derived from neurons and glia play a variety range of roles such as supporting cells, regulating cellular signaling, coordinating synaptogenesis, and synaptic activity (Dityatev and Schachner, 2003; Washbourne et al., 2004; Dityatev and Fellin, 2008; Lee et al., 2008). Collagens are part of ECM proteins that play active roles during the neurodevelopment and neurodegeneration (Fox, 2008; Hubert et al., 2009). However, few studies have dissected the consequential molecular mechanism of collagens in response to the stress conditions in the central nervous system.

Collagen VI is one of the 28 collagen protein families that composed of six subunits (Col6α1~6) encoded by separate genes (*Col6a1~6*). Col6α1, Col6α2, and Col6α3 subunits assemble in 1:1:1 ratio to form monomers and further secrete to extracellular space where they assemble into microfibrils (Bruns et al., 1986; Schreier et al., 1987; Kielty et al., 1992). Col6α4, Col6α5, and Col6α6 are newly identified as members in collagen VI family, but their structural and functional roles remain unclear (Fitzgerald et al., 2008). Similar to many other molecules in ECM, collagen VI regulates cell survival and promotes tumor progression via binding to cell surface proteins and alternating downstream signaling cascades (Kuo et al., 1997; Howell and Doane, 1998; Ruehl et al., 1999; Milner and Campbell, 2002; Iyengar et al., 2005). The mutations on *Col6* genes result in muscular diseases Bethlem myopathy and Ullrich congenital muscular dystrophy (Lampe and Bushby, 2005; Lampe et al., 2008). However, the role of collagen VI in the central nervous system is yet little understood.

Apoptosis is the process of programmed cell death, which involves a series of morphological changes, including cell detachment, cell shrinkage, mitochondria leakage, chromatin condensation, and DNA fragmentation (Kanazawa, 2001). This process is controlled by the balance between multiple pro-apoptotic and anti-apoptotic signaling pathways, which may originate either extracellularly or intracellularly. Two of the key signaling molecules regulating this balance are Akt/phosphoinositide 3-kinase (PI3K) and Jun N-terminal kinase (JNK) cascades. Activation of Akt through phosphorylation has an anti-apoptotic role in a variety of tissue culture models against the withdrawal of growth factors, ultraviolet (UV) irradiation, matrix detachment, cell cycle disturbance, and DNA damages (Datta et al., 1997, 1999; Khwaja et al., 1997; Brazil et al., 2002; Burke, 2007; Parcellier et al., 2008). In contrast, activation of JNK through phosphorylation has a pro-apoptotic role under many different types of stresses, such as UV irradiation (Dérijard et al., 1994; Caridad and Karin, 1996; Ro-

*Corresponding author. Tel: +886-2-2826-7905; fax: +886-2-2827-3123.
E-mail address: hjcheng@ym.edu.tw (I. H. Cheng).

Abbreviations: DAPI, 4′-6-diamidino-2-phenylindole; ECM, extracellular matrix; GAPDH, glyceraldehyde 3-phosphate dehydrogenase; GFAP, glial fibrillary acidic protein; JNK, jun N-terminal kinase; MAP-2, microtubule-associated protein-2; PBS, phosphate buffered saline; PI3K, phosphatidylinositol 3-kinases; qPCR, quantitative polymerase chain reaction; TUNEL, terminal deoxynucleotidyl transferase dUTP nick end labeling; UV, ultraviolet.

0306-4522/11 $ - see front matter
doi:10.1016/j.neuroscience.2011.03.057

sette and Karin, 1996; Davis, 2000; Dhanasekaran and Reddy, 2008). Inhibition of JNK activity results in attenuation of apoptosis in UV irradiated cells (Zhang et al., 2008; Kim et al., 2009).

To determine the role of ECM proteins on neurons under stress conditions, we surveyed the level of known ECM proteins after UV irradiation. In this report, we described that increased levels of *Col6a1-3* mRNA and collagen VI protein in neurons after UV irradiation. Soluble collagen VI may have a functional role in neuronal survival through the activating Akt/PI3K and inhibiting JNK signaling pathway.

EXPERIMENTAL PROCEDURES

Primary neuronal cultures

The pregnant C57BL/6JNarl mice were purchased from National Laboratory Animal Center (NLAC, Taipei, Taiwan) with the approval of the Institutional Animal Care and Use Committee at National Yang Ming University. Primary hippocampal neuronal cultures, in which more than 95% of cells were immunoreactive for microtubule-associated protein-2 (MAP-2, see Fig. 3), were generated from embryonic day 19 or post-natal day 0 mice as described (Chu et al., 2009). After growing 8 days *in vitro*, primary neurons were treated with collagen VI (354261, BD Biosciences, USA) or collagen IV (354245, BD Biosciences, Bedford, MA, USA) 2 h before UV irradiation. UV irradiation was carried out using UVC lamp emitting maximally at 253.7 nm (Philip, Eindhoven, Netherlands) for 20 min in collagen VI containing medium. UV irradiance was measured using a UVX radiometer UVX-25 (Ultraviolet Products, Rockford, IL, USA) before each use.

Quantitative polymerase chain reaction (qPCR)

Primary neuronal cultures were grown on six-well plates at 4×10^6 cells/well. After treatments, neurons were harvested with 0.05% trypsin and centrifuged for 20 s at 4700×*g*, and their RNA was isolated using the Total RNA Mini Kit (RB050, Geneaid, Taiwan). RNA concentration was determined by NanoDrop Spectrophotometer (ND-1000, Thermo, Rockford, IL, USA). Total RNA was reverse transcribed with oligo(dT) primers and Moloney Murine leukemia virus reverse transcriptase (RT80110K, Epicentre, Madison, WI, USA). The expression level of different *Col6a1-3* genes relative to glyceraldehyde 3-phosphate dehydrogenase (GAPDH) was determined by SYBR Green dye (04673484001, Roche, Indianapolis, IN, USA) and an ABI StepOne plus real-time PCR machine (Applied Biosystems, Foster City, CA, USA). The following primers were used: mouse *Col6a1* (forward, 5′-TGCCCTGTGGATCTATTCTTCG-3′; reverse, 5′-CTGTCTCTCAGGTTGTCAATG-3′), mouse *Col6a2* (forward, 5′-CATCTCACCCCAGGAGCAGGAA-3′; reverse, 5′-TACACGTTGACTGGGCAGTCGG-3′), mouse *Col6a3* (forward, 5′-AACCCTCCACATACTGCTAATTC-3′; reverse, 5′-TCGTTGTCACTGGCTTCATT-3′), mouse *GAPDH* (forward, 5′-GGGAAGCCCATCACCATCTT-3′; reverse, 5′-GCCTTCTCCATGGTGGTGAA-3′), mouse *Col1a1* (forward, 5′-ATGGATAGGGACTTGTGTGAA-3′; reverse, 5′-CTTCTTAAATAGCACCTTCAG-3′), mouse *Col4a1* (forward, 5′-CAAATGCTTACAGCTTTTGGC-3′; reverse, 5′-TCTTCTCATGCACACTTGGC-3′).

Immunoblotting

Primary neuronal cultures were grown on six-well plates at 4×10^6 cells/well. To detect collagen VI protein level, culture media were collected at 0, 2, and 4 h after UV irradiation. For dot blot analysis, 20 μl of culture media was spotted on pre-soaked nitrocellulose membrane five times and probed with anti-collagen VI antibody (ab6588, Abcam, Cambridge, UK). To detect Akt and JNK levels, neurons were collected at 30 min after irradiation and lysed in ice-cold radioimmunoprecipitation assay (RIPA) buffer (50 mM Tris pH 7.5, 150 mM NaCl, 10 mM EDTA, 1% NP-40, 0.1% SDS) containing phosphatase inhibitor (04906845001, Roche, Indianapolis, IN, USA) and protease inhibitor (04693116001, Roche, USA). The cell lysates were agitated at 4 °C for 30 min and then centrifuged at 16100×*g* at 4 °C for 10 min. The protein concentration was measured by Bradford assay (PAK500, Strong Biotech Corp, Taipei, Taiwan). Protein samples (66.5 μg) were heated at 95 °C for 10 min and separated in 10% SDS-PAGE. Western blotting was performed using anti-phospho-Akt at Ser-473 (9271, Cell signaling, Beverly, MA, USA), anti-total Akt (9272, Cell Signaling, Beverly, MA, USA), anti-phospho-JNK at Thr183/Tyr185 (9251, Cell signaling, USA), anti-total Akt (9252, Cell Signaling, Beverly, MA, USA), and anti-actin (MAB1501, Millipore, Billerica, MA, USA) antibodies. Immunoblot signals were developed by chemiluminescent HRP substrate (WBKLS0500, Millipore, Billerica, MA, USA) and detected with the Fujifilm Luminescence/Fluorescence Imaging System (LAS-4000, Fujifilm, Tokyo, Japan). Multi Gauge v3.0 was used for image acquisition and data analysis.

Immunocytochemistry

Primary neurons were grown on 12 mm coverslips in 24-well plates at 2.5×10^5 cells/well. Immediately after UV and collagen VI treatments, neurons were fixed in 4% paraformaldehyde for 60 min at room temperature. Fixed neurons were permeabilized with 0.1% Triton X-100 in phosphate buffered saline (PBS, 137 mM NaCl, 2.7 mM KCl, 10 mM Na_2HPO_4, 2 mM KH_2PO_4, pH of 7.4) for 10 min, blocked with 10% fetal bovine serum (04001-1A, Biological Inc., Taipei, Taiwan), and incubated overnight at 4 °C with the primary antibodies, including monoclonal mouse anti-MAP-2 (MAB378, Millipore, Billerica, MA, USA), and polyclonal rabbit anti-glial fibrillary acidic protein (GFAP, Z0334, DAKO, Glostrup, Denmark). Neurons were then rinsed with cold PBS and incubated with either Texas-Red-conjugated goat anti-mouse IgG (103007, AbD Serotec, Kidlington, UK) or FITC-conjugated goat anti-rabbit IgG (AP132F, Millipore, Billerica, MA, USA) for 1 h. The coverslips were mounted with VECTASHIELD® plus 4′-6-Diamidino-2-phenylindole (DAPI, H-1200, Vector Lab Inc., Burlingame, CA, USA). Omission of primary antibody served as negative controls. Fluorescent images of cells were captured on a CCD camera (DP50) mounted on an Olympus fluorescence microscope (BX-52, Olympus, Tokyo, Japan) equipped with a mercury arc lamp.

Terminal deoxynucleotidyl transferase dUTP nick end labeling (TUNEL) assay

TUNEL assay was performed using the DeadEnd™ Fluorimetric TUNEL System (G3250, Promega, Madison, WI, USA). Primary neurons were cultured and treated in the same condition as immunocytochemistry experiments. The TUNEL staining was performed as described in Promega manual. The number of TUNEL-positive cells were counted in three different 10× fields per sample using ImageJ software (free downloaded from NIH website: http://rsbweb.nih.gov/ij/).

MTT assay

Primary neuronal cultures were seeded in 96-well plates (10^5 cells/well). 2 h after all treatments, 3-(4,5-dimethylthiazol-2-yl)-2,5-diphenyltetrazolium bromide (MTT, 298-93-1, Bio Basic Inc, Taipei, Taiwan) was added to the medium (0.5 mg/ml) and incubated at 37 °C. After 4 h, 100 μl of lysis buffer containing 10% SDS and 20 mM HCl was applied to each well and incubated at 37 °C overnight to dissolve the formazan crystals. The absorbance at wavelength 570 nm in each well was measured on a

microenzyme-linked immunosorbent assay (ELISA) reader (TECAN, Männedorf, Switzerland).

NeurotoxQ

NeurotoxQ was implemented as an ImageJ macro. In order to perform all necessary operations, an additional ImageJ plugins "particle remover" (http://rsb.info.nih.gov/ij/plugins/particle-remover.html) was incorporated. NeurotoxQ pre-processes the image using edge detection and background correction with user-defined parameters. To detect edges, the original image was subtracted from the image that had been smoothened by a Gaussian kernel. Uneven background was corrected using the "subtract background" function with a rolling ball radius of 50°pixels. Neuronal cell bodies were extracted from the pre-processed image using an open operation (minimum filter followed by maximum filter). The image with extracted neuronal cell bodies was binarized for quantification. The pre-processed image was also binarized, cell debris and small particles were removed via user-defined size criterion. The resulting "clean" image was skeletonized to reduce all objects into single pixel wide skeletons. Neuronal cell bodies were subtracted from the skeleton image to obtain the neurite length. In addition, neuronal cell bodies were subtracted from the "clean" image to obtain the neurite area. The color combined images were generated by combining the binarized neurite length image, the original image, and the binarized neuronal cell body image. NeurotoxQ was available for free download at http://life.nctu.edu.tw/~microtubule/macros.html (Username: neurotoxQ, Password: microtubule).

Statistics

All results were displayed as mean±SEM. Statistical analyses were carried out with SPSS (IBM SPSS, Chicago, IL, USA). Data were analyzed using one-way ANOVA and Student-Newman-Keuls post-test. *P*-values lower than 0.05 were considered significant.

RESULTS

UV irradiation up-regulates collagen VI gene expression after UV irradiation

The composition of ECM proteins could play a detrimental role in controlling pro- or anti-apoptotic signaling pathways under stress conditions. This study was aimed to identify the alteration of ECM genes expression after UV irradiation in neurons, and to determine the role of these genes in apoptosis. After 192 J/m^2 UV irradiation, mouse primary hippocampal neurons were harvested after 30 min for measuring mRNA levels by qPCR. One of the most up-regulated mRNA encoding ECM proteins was the *Col6* gene family. Relative to no UV irradiated control group, expression level of mRNA encoding the α1 subunit (*Col6a1*) had 3.0-fold increase; the mRNA encoding α2 subunit (*Col6a2*) had 3.9-fold increase; the mRNA encoding α3 subunit (*Col6a3*) had 9.7-fold increase ($P<0.05$ for all three genes in UV vs. no UV groups (Fig. 1A). However, the expression levels of mRNA encoding other collagen genes, such as *Col1a1* and *Col4a1*, did not have significant difference after UV irradiation.

Because the increase of mRNA level does not necessary lead to the increase in protein level, we therefore also measured the amount of collagen VI protein in culture medium at 0, 2, and 4 h after UV irradiation. Relative to 0 h group, the level of collagen VI protein increased 2.2-fold at 2 h and increased three-fold at 4 h after irradiation (both $P<0.05$, Fig. 1B). This expression analysis revealed that *Col6* mRNA and collagen VI protein are quickly up-regulated after UV irradiation.

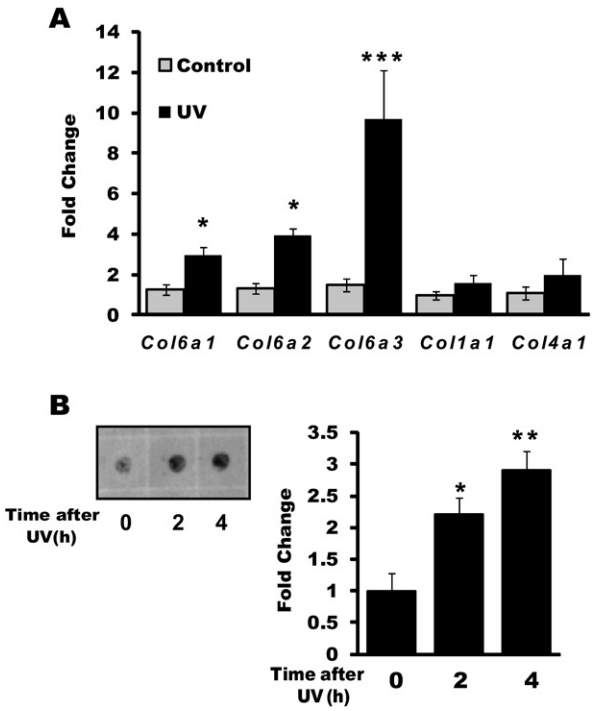

Fig. 1. Increase level of collagen VI after 192 J/m^2 UV irradiation in primary hippocampal neurons. (A) The expression levels of *Col6a1*, *Col6a2,* and *Col6a3* mRNAs (encoding collagen VIα1, α2, and α3 subunits) at 30 min after UV irradiation were monitored by qPCR. *Col1a1* and *Col4a1* mRNAs were also measured. The mean *Col/Gapdh* mRNA ratios in no UV irradiated group of each gene were defined as 1. Black bars represent data from UV irradiated neurons; grey bar represents data from no UV control neurons. (B) The levels of collagen VI protein in the culture media at 0, 2, and 4 h after irradiation were monitored by dot blot. The average density of collagen VI at time 0 was defined as 1. The results were averaged from three independent experiments. $n=3$ in each condition per experiment. * $P<0.05$, ** $P<0.01$, and *** $P<0.001$ versus no UV control.

Collagen VI protects neurons against UV irradiation

The up-regulated collagen VI may serve as either an anti-apoptotic factor to protect neurons against UV, or a pro-apoptotic mediator to activate UV-induced cell death. To elucidate the role of collagen VI, we investigated if exogenous applying extra soluble collagen VI protein in the medium can make neurons more resistant or sensitive to UV irradiation. Primary neuronal cultures were pre-treated with media containing 0, 25 or 50 nM of purified human collagen VI protein for 2 h, and then exposed to 192 J/m^2 UV. The appearance of DNA strand fragmentation labeling by TUNEL assay is one of the hallmarks of apoptotic cells. We therefore labeled treated cells with TUNEL and calculated the ratio of TUNEL positive neurons as: {number of TUNEL positive cells (pink)/number of DAPI stained cells (blue)}×100%. The ratio of TUNEL positive neurons were five-folds higher in UV irradiated culture than no UV control culture ($P<0.05$; Fig. 2A, B, F). However, under the same dose of UV, the ratio of TUNEL

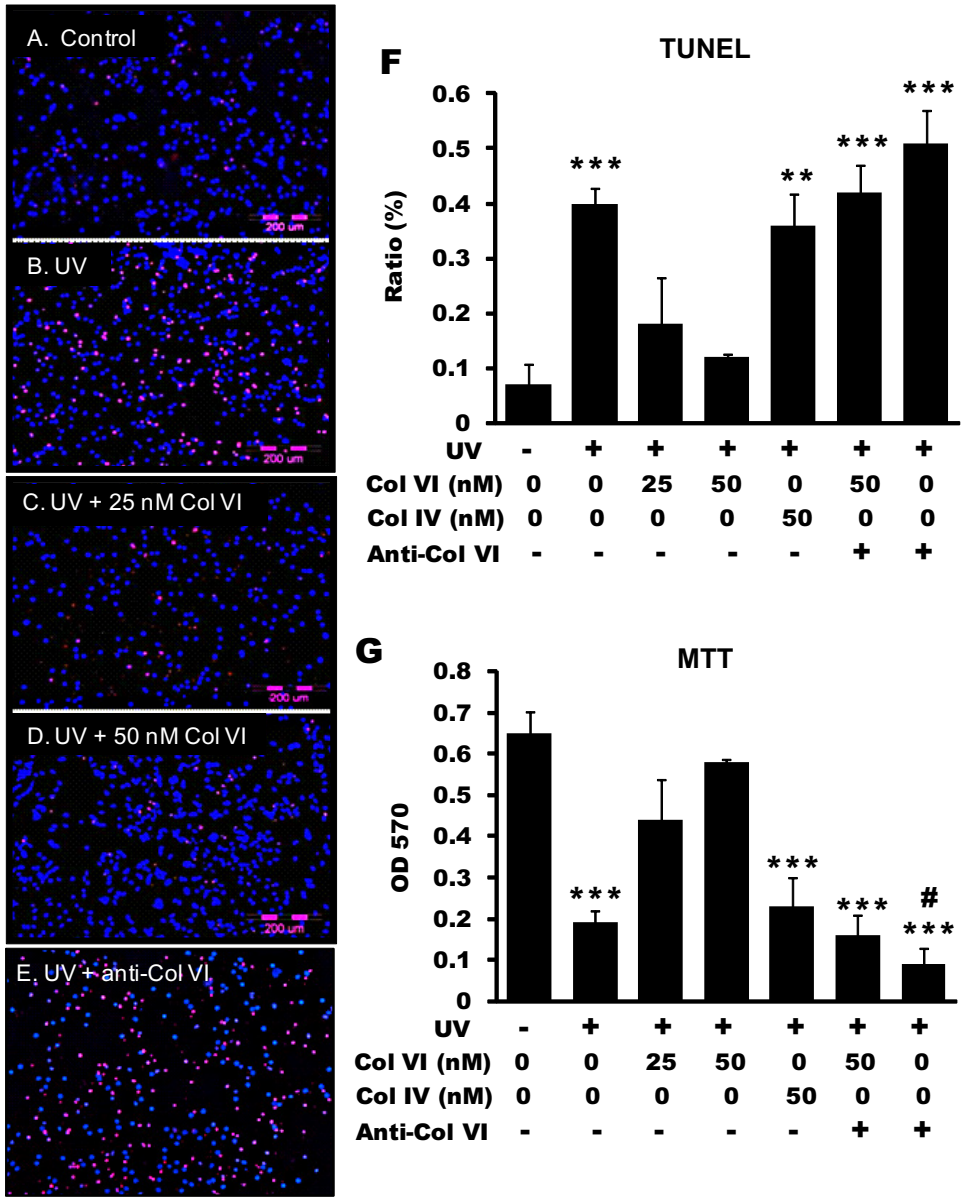

Fig. 2. Collagen VI rescued UV-induced DNA damage in TUNEL assay and mitochondria dysfunction in MTT assay. Primary neurons with or without 2 h collagen VI pre-treatment were irradiated with 192 J/m^2 UV. (A–E) Representative TUNEL images of neuronal cultures with following treatments: control (A), UV (B), UV+25 nM collagen VI (C), UV+50 nM collagen VI (D), UV+250 nM anti-collagen VI antibody (E). Blue, DAPI staining for nuclei; pink, TUNEL positive nuclei. Scale bar represents 200 μm. (F) TUNEL positive ratios were calculated as: (number of TUNEL positive cells/number of nuclei) $\times$100%. Three pictures were taken from each well, and four repeated wells were performed in each condition per experiment. The results were averaged from four independent experiments. (G) Mitochondria metabolic function was determined by MTT assay with the mean OD570 readings. The results were averaged from five independent experiments. n=8 for each group per experiment. ** $P<0.01$, *** $P<0.001$ versus no UV control. $^{\#}$ $P<0.05$ versus UV only group.

positive neurons decreased 70% in 25 nM collagen VI-treated cultures, and decreased 80% in 50 nM collagen VI-treated cultures (both $P<0.05$ vs. UV-irradiated group (Fig. 2C, D, F). Because pre-treating neurons with soluble collagen VI make neurons more resistant to UV induced apoptosis, collagen VI may have a protective role in neurons.

In addition to DNA breakage, we also investigated whether collagen VI treatment can rescue the mitochondria metabolic dysfunction induced by UV irradiation. We determined the mitochondria activity of primary neurons by MTT assay and compared the mean OD570 absorbance value to represent the mitochondria activity of live cells. Similar to the result from TUNEL assay, we found that mitochondria activities were impaired after UV irradiation ($P<0.01$ vs. no UV group) but could be rescued by collagen VI pre-treatment (Fig. 2G, $P<0.05$).

One of the possible explanations for the protective effect of collagen VI is that the presence of extra 50 nM of protein in the culture medium may block UV irradiation. To test this possibility, 50 nM of soluble human collagen IV protein was also added into medium as control. In contrast to collagen VI treatment, pre-treating neurons with collagen IV failed to res-

cue DNA damage and mitochondria dysfunction induced by UV irradiation (Fig. 2F, G). To further confirm the essential role of collagen VI, we also added 250 nM of anti-collagen VI antibody to naturalize the effect of both exogenous and endogenous collagen VI. The protective effect of 50 nM exogenous collagen VI was diminished in the presence of specific antibody in both TUNEL and MTT assays (Fig. 2F, G). After naturalizing endogenous collagen VI, these cells had a significantly worse mitochondria dysfunction in MTT assay (Fig. 2G, $P<0.05$ vs. UV group), but only a trend toward more DNA damage in TUNEL assay (Fig. 2E, F, $P=0.07$ vs. UV group). These results suggested that this protective effect is collagen VI specific.

During the apoptosis process, shrinkage of neurites and somas are commonly seen and easy to detect (Kanazawa, 2001). To quantify these morphological alterations, nevertheless, manual measurement is extremely time consuming and biased. We therefore developed an ImageJ-based morphology quantification algorithm, NeurotoxQ, which provides automatic measurements of the following neuronal morphological parameters: (1) the average length of the neurite segments of each neuron, and (2) the average size of each neuron cell body (soma), (3) the number of neurons.

To examine whether collagen VI treatments can rescue the alteration of cell number and morphology after UV irradiation, primary neuronal cultures were pre-treated with 50 nM of collagen VI for 2 h before UV irradiation. These cells were immunolabeled with neuron specific marker MAP-2 (red), and their nuclei were labeled with a nuclei dye DAPI (blue) (Fig. 3A–D). After UV irradiation, the average neurite length per neuron was >50% shorter than no UV control ($P<0.01$, Fig. 3A, B, E). However, under the same dosage of UV, the average neurite length was 1.5- and 1.7-fold longer in 25 and 50 nM collagen VI-treated cultures (both $P<0.05$ vs. after UV-irradiated group, Fig. 3C, D, E). Nevertheless, there was no significant difference in the average size of soma with or without UV irradiation and collagen VI treatment (Fig. 3F). In addition, the number of MAP positive neurons per image field did not have significant difference (Fig. 3G). Therefore, the average length of neurites, but not the size of soma, was consistent with the data from TUNEL and MTT assays indicating that pre-treating cultures with collagen VI rescues neurons from UV-induced cell damage.

To evaluate our algorithm, we compared neurite length determined manually using NeuronJ with that obtained using NeurotoxQ. Sixteen images of mouse hippocampal neurons were used to evaluate NeurotoxQ (Fig. 4A). NeurotoxQ-produced neurite tracings were highly correlated (Pearson's correlation coefficients $R=0.95$) (Fig. 4B) and statistically indistinguishable ($P=0.2275$ from the two-tailed Student's *t*-test) from manual tracings.

Collagen VI alters apoptotic signaling pathways

Because soluble collagen VI made neurons more resistant to UV irradiation, we speculated that collagen VI may bind to unidentified cell surface protein and alter survival-related signaling pathways. In most cell types, the balance of pro-apoptotic and anti-apoptotic signals determines cell fate under stress conditions. To decipher the molecular paths that mediate the protective effect of collagen VI, we used Western blot to monitor phosphorylation states of Akt and JNK, whose activities are critical for regulating cell survival/death upon UV irradiation. After UV irradiation, the ratio of phosphorylated Akt protein was not significantly altered in primary neurons. However, under the same dosage of UV, the ratio of phosphorylated Akt increased 1.6-folds with 25 nM collagen VI treatment, and increased 1.8-folds with 50 nM collagen VI treatment (both $P<0.05$ vs. UV irradiated group, Fig. 5A, B). In contrast, the ratio of phosphorylated JNK protein increased 2.6-fold after UV irradiation ($P<0.05$ vs. no UV control, Fig. 5A, C). Under the same dosage of UV, ratio of phosphorylated JNK decreased 49% in 25 nM collagen VI treated cells, and decreased 60% in 50 nM collagen VI treated cells (both $P<0.05$ vs. UV-irradiated group, Fig. 5A, C). In summary, soluble collagen VI could stimulate Akt and inhibit JNK phosphorylation in UV-irradiated neurons.

Based on the Western blot result and well-established anti-apoptotic role of Akt, we hypothesized that collagen VI may stimulate Akt/PI3K signaling pathway to protect neurons against UV irradiation. To further confirm the role of Akt/PI3K, primary neuronal cultures were co-treated with 50 nM of collagen VI together with 50 μM Akt/PI3K inhibitor LY294002 for 2 h before UV irradiation. Treating neurons with collagen VI alone increased the ratio of phosphorylated Akt, but treating neurons with collagen VI and LY294002 together lowered the ratio of phosphorylated Akt to untreated level (Fig. 6F). We determined the degree of damage under these treatments by neurite length alteration and cell counts. Similar to our finding in Fig. 3, we found that UV irradiation reduced the average length of neurites, but collagen VI treatment rescued this damage effect (Fig. 6A–C, G). Under the same dosage of UV and collagen VI, Akt/PI3K inhibitor treated neurons had shorter neurite length than no inhibitor treated neurons ($P<0.05$ vs. collagen VI only, Fig. 6C, D, G). Without UV irradiation, treating neurons with collagen VI and Akt/PI3K inhibitor did not affect neurite length. Nevertheless, there was no significant difference in the total number of neurons under all treatments (Fig. 6H).

Furthermore, we investigated the effect of collagen VI, Akt/PI3K inhibitor and the combination treatments on the UV-induced DNA damage and mitochondria dysfunction. After UV irradiation, neuronal culture co-treated with Akt/PI3K inhibitor and collagen VI had higher ratio of damaged cells than collagen VI only culture (both $P<0.05$, Fig. 7). In the absence of collagen VI, neurons with or without Akt/PI3K inhibitor treatment did not have significant difference in cell survival under the same does of UV irradiation. In the absence of UV irradiation, treating neurons with Akt/PI3K inhibitor alone or in combination with collagen VI did not affect the cell survival (Fig. 7). These results support the notion that Akt/PI3K signaling plays an anti-apoptotic role in the collagen VI-dependent protection of neurons against UV-induced apoptosis.

DISCUSSION

In this study, we found that neurons have increased *Col6a1*, *Col6a2*, and *Col6a3* mRNA levels along with se-

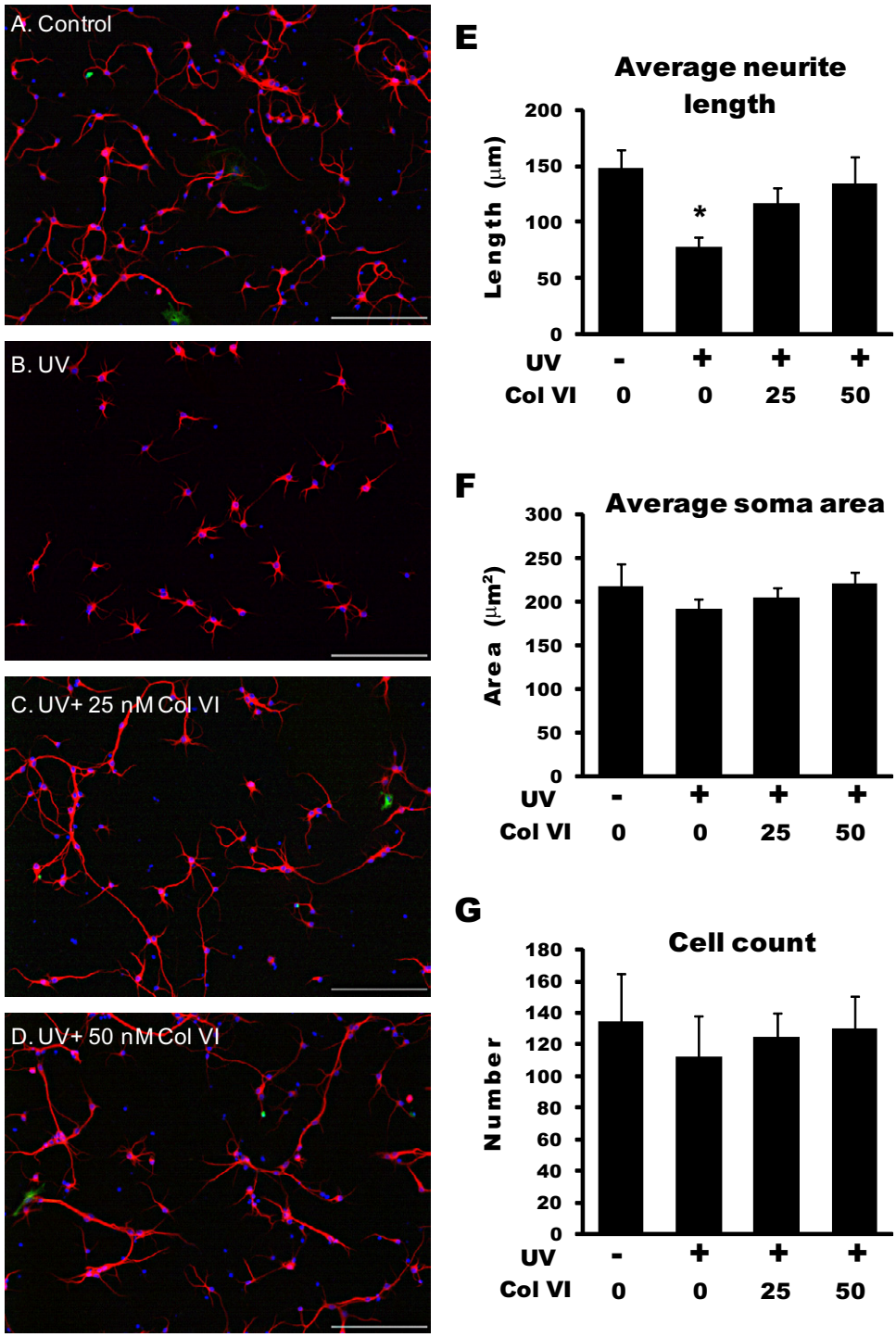

Fig. 3. Collagen VI rescued UV-induced neurite shrinkage. Primary neurons with or without 2 h collagen VI pre-treatment were irradiated with 192 J/m^2 UV. (A–D) Representative images of MAP-2 positive neurons with following treatments: control (A), UV (B), UV+25 nM collagen VI (C), UV+50 nM collagen VI (D). Blue, DAPI staining for nuclei; green, GFAP staining for astrocytes; red, MAP-2 staining for neurons. Scale bar represents 200 μm. (E–G) Quantification of average neurite length (E), average soma area (F), and total cell count (G) of MAP-2 positive neurons determined by NeurotoxQ. The results were averaged from four independent experiments. Three pictures were taken from each well, and three to six repeated wells were performed in each condition per experiment. * $P<0.05$ versus no UV control.

creted collagen VI protein level after UV irradiation. UV usually causes multiple cellular damages and induces apoptosis process in many types of cells (Lu and Lane, 1993). To determine whether the up-regulation of collagen VI plays a protective or detrimental role after UV irradiation, we exogenously applied soluble collagen VI into the

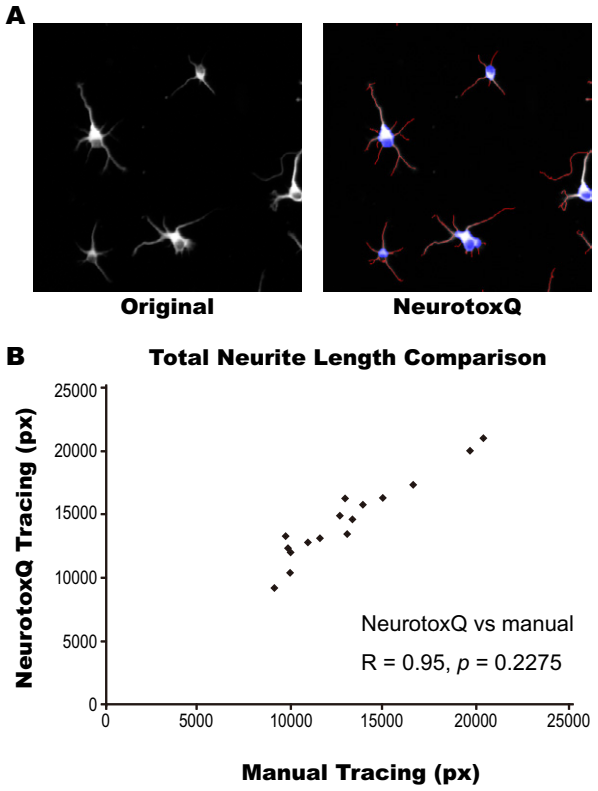

Fig. 4. NeurotoxQ produced accurate neurite length estimation in images of primary hippocampal neurons. (A) Example image of mouse hippocampal neurons analyzed by NeurotoxQ. Neurite tracings are shown in red and somas are in blue in analyzed images. (B) Sixteen mouse hippocampal neuron images manually traced or automatically traced using NeurotoxQ were compared. Total neurite length (in pixels) obtained by manual tracing is plotted on the X-axis, and total neurite length obtained by NeurotoxQ is plotted on the Y-axis. Pearson's correlation coefficient and two-tailed Student's *t*-test result are indicated.

primary neuronal culture medium. Assays for DNA damage, mitochondria dysfunction, and cell morphology indicated that the higher concentration of soluble collagen VI protein made neurons more resistant to UV irradiation. In addition, we demonstrated that collagen VI-treated neurons have higher Akt activity and lower JNK activity after UV irradiation. Inhibiting Akt/PI3K activity diminished the protective effect of collagen VI. Our findings suggested that collagen VI may enhance neuronal survival after UV irradiation through inducing Akt/PI3K anti-apoptotic pathway.

Expression of *Col6* genes are increased after UV damage

After neuronal damage by UV irradiation, we found that both collagen VI mRNA and protein levels were significantly up-regulated. Although collagen VI protein is undetectable inside the neurons, it has significantly higher level in culture medium after UV irradiation, which is consistent with its role as an extracellular protein. Similarly, when neurons expose to amyloid-β peptide (Aβ), the primary toxin causing Alzheimer's disease, *Col6a1* gene expression is up-regulated through the TGF-β/Smad3 pathway to make neurons more resistant to Aβ (Cheng et al., 2009). The dynamic expression of *Col6* gene family has been founded in multiple types of cells under normal and pathogenic conditions (Hatamochi et al., 1989; Adriaenssens et al., 2009). For example, during tumor progression, *Col6* genes are up-regulated to promote survival of tumor cells through the β-catenin/TCF signaling pathway (Sherman-Baust et al., 2003; Iyengar et al., 2005). Therefore, our result is consistent with others suggesting that up-regulating *Col6* gene expression could be a general response under stress condition in multiple types of cells including neurons.

Soluble collagen VI protects neurons against UV damage

Collagen VI protein has important roles in the control of DNA synthesis, cell survival, proliferation, and metabolism of normal and transformed cells (Ruehl et al., 1999; Ruhl et al., 1999; Irwin et al., 2003; Sherman-Baust et al., 2003; Iyengar et al., 2005; Cheng et al., 2009; Khan et al., 2009). In contrast, *Col6a1* knockout mouse and zebrafish have mitochondrial dysfunction, ultrastructural defects, and increased incidence of apoptosis in myofibers (Palma et al., 2009; Telfer et al., 2010). Furthermore, primary neurons generated from *Col6a1* knockout mice is more sensitive to Aβ (Cheng et al., 2009). Our result agrees with others suggesting that collagen VI could have a pro-survival role in neurons.

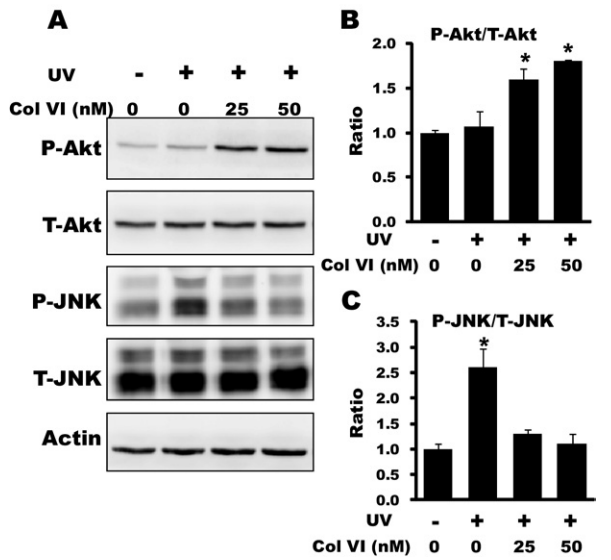

Fig. 5. Phosphorylation states of Akt and JNK were altered after collagen VI treatment. Primary neurons with or without 2 h collagen VI pre-treatment were irradiated with 192 J/m^2 UV. (A) Representative Western blot images of phosphorylated Akt (P-Akt), total Akt (T-Akt), phosphorylated JNK (P-JNK), and total JNK (T-JNK) in neurons with UV and collagen VI treatments. Immediately after these treatments, neurons were lysed in RIPA buffer and analyzed in 10% SDS-PAGE. Actin was served as loading control. (B, C) The phosphorylation ratios of Akt (B) and JNK (C) were calculated as (intensity of phosphorylated protein)/(intensity of total protein). The mean phosphorylation ratios in no UV irradiated group of each kinase were defined as 1. The results were averaged from three independent experiments. Three Western blots were performed per experiment. * $P<0.05$ versus no UV control group.

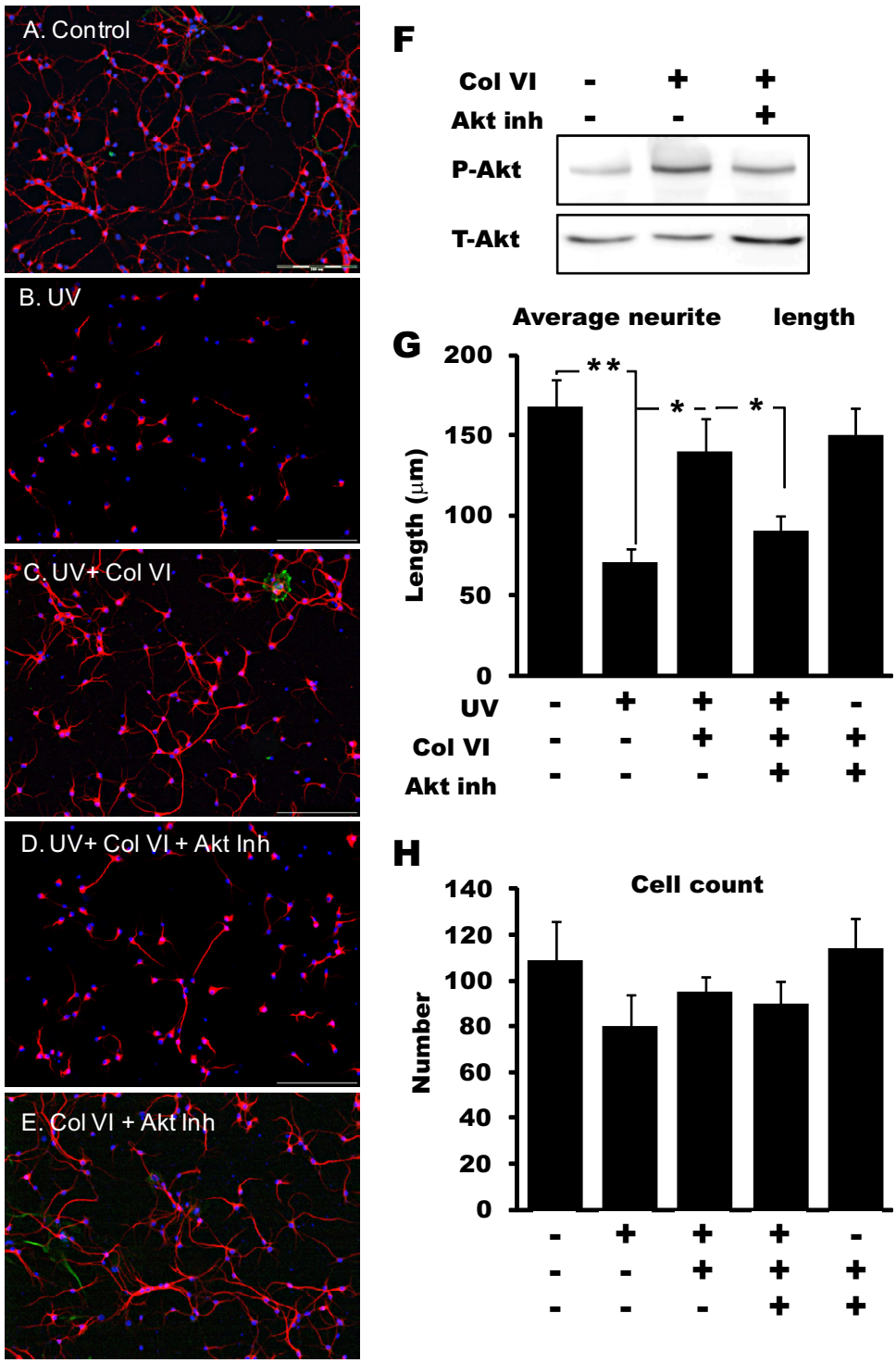

Fig. 6. Inhibition of Akt/PI3K activity diminished the anti-apoptotic effect of collagen VI in morphology study. (A–E) Representative images of the morphology of MAP-2 labeled neurons with following treatments: control (A), UV (B), UV+50 nM collagen VI (C), UV+50 nM collagen VI+Akt inhibitor (D), 50 nM collagen VI+Akt inhibitor (E). Blue, DAPI staining for nuclei; green, GFAP staining for astrocytes; red, MAP-2 staining for neurons. Scale bar represents 200 μm. (F) Representative Western blot images of phosphorylated Akt (P-Akt) and total Akt (T-Akt). The phosphorylation ratio of Akt was partially reduced after treating with inhibitor. (G, H) Average neurite length (G) and cell count (H) under different treatments were determined by NeurotoxQ as described in Fig. 3. The results were averaged from three independent experiments. Three pictures were taken from each well, and three to six repeated wells were performed in each condition per experiment. * $P<0.05$, ** $P<0.01$ between each comparison group.

Collagen VI α1–3 subunits are believed to be stable as a heterotrimeric chain complex (Bruns et al., 1986; Kielty et al., 1992), but it remains possible that each subunit has specific functions. The collagen VI used in this study is

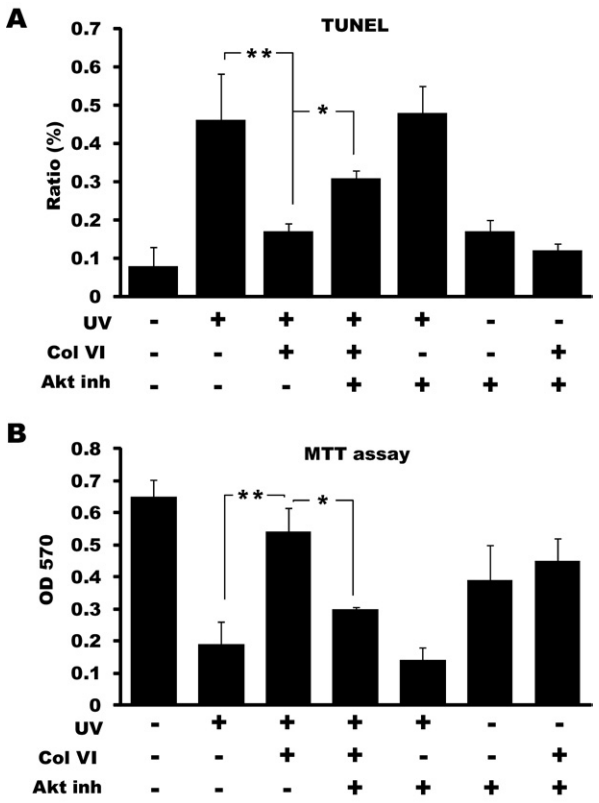

Fig. 7. Inhibition of Akt/PI3K activity diminished the anti-apoptotic effect of collagen VI in TUNEL and MTT assays. (A) Percent DNA damage under different treatments was determined by TUNEL assay. Three pictures were taken from each well, and three to eight repeated wells were performed in each condition per experiment. (B) Cell metabolic impairment under different treatment was determined by MTT assay. $n=8$ for each group per experiment. Both results were averaged from three independent experiments. * $P<0.05$, ** $P<0.01$ between each comparison group.

purified from human placenta and contains all subunits. Whether individual subunit of collagen VI also has anti-apoptosis effects remains unclear. Our attempt for using siRNA to knockdown *Col6* genes altered the morphology of primary neurons even without any treatment. We hence were unable to confirm the specify role of each collagen VI subunit.

Although the role of collagen VI on cell survival is evidenced in several studies, the mechanism by which collagen VI protects neurons remains unclear. Collagen VI has been shown to protect neurons through trapping Aβ into larger aggregates thus avoiding Aβ binding onto neurons (Cheng et al., 2009). In this study, it is also possible that collagen VI physically traps UV-induced toxins such as Aβ. Nevertheless, adding other type of filbrogenic collagen protein into media did not reduce UV-induced damage. Therefore, this collagen VI specific protective mechanism may be caused by collagen VI-toxins specific interaction or collagen VI-dependent anti-apoptotic signaling. In addition, we decided to add soluble collagen VI into culture media but not to coat it on the culture plates because primary neurons did not grow well on collagen VI coated surface. Therefore, this protective effect is less likely due to the enhancement of neuronal adhesion but more likely due to the activation of the anti-apoptotic signaling.

Collagen VI alters Akt/PI3K signaling pathway

We identified that the activation of Akt/PI3K pathway may involve in collagen VI dependent protective effect in primary neurons. Phosphorylation of Akt was induced in neurons after collagen VI treatment, and inhibition of Akt/PI3K signaling pathway diminished the protective effect of collagen VI against UV irradiation. Akt/PI3K is highly expressed in the brain and many other tissues, and is known as one of the major signaling molecules for cell proliferation and survival mediated by extracellular stimuli (Brunet et al., 2001; Brazil et al., 2002; Parcellier et al., 2008). Akt/PI3K activation is known to increase the cell resistance to UV irradiation via inhibiting of JNK activation in several types of cells (Sunayama et al., 2005; Kim et al., 2009). Similar to our findings, collagen VI can also increase phosphorylation of Akt/PI3K to promote its growth-stimulatory and pro-survival effects of tumor cells (Iyengar et al., 2005).

NeurotoxQ, a free, automatic morphological quantification program

Improvement of tools to study cellular and molecular biology is playing an increasingly important role in assisting researchers to study the mechanisms of diseases or screening novel drugs. Neuronal morphological changes after neuronal damages are typically quantified by manual examination. This kind of quantification is time consuming, inconsistent, and highly subjective. Programs for high-throughput screening are not always easy to adopt for small scale laboratory use (Zhang et al., 2007; Daub et al., 2009). The utilization of NeurotoxQ allows rapid, consistent, and objective quantification of neuronal cell body, neurite area, neurite length, and neurite thickness using image processing principles. We benchmarked NeurotoxQ and found that a typical 1×10^6-pixel image acquired using a $10\times$ objective takes roughly 15 s to complete. This is a significant improvement over another ImageJ-based automatic tracing algorithm which takes 2~3 min (Narro et al., 2007) or a computer-aided manual tracing algorithm which can take hours (Meijering et al., 2004). However, it is important to note that the result from NeurotoxQ quantification is on a per image field basis. Due to the complexity of the neuronal network, it is extremely difficult, if not impossible, to distinguish neurites originated from different neurons; this prevents us from developing an algorithm that can generate quantitative data on a per cell basis. As a result, it is crucial to normalize the neurite length or neurite area using neuronal cell body if one wishes to compare results on a per cell basis. In addition, NeurotoxQ cannot operate on images acquired using high magnification objectives (higher than $20\times$). This is due to the skeletonize operation utilized. When high magnification images are processed, skeletonize operation produces tree-like branches within thick neu-

rites and hence results in an over-estimation of the neurite length.

Acknowledgments——This work was supported by Taiwan National Health Research Institutes grant NHRI-EX98-9816NC, Taiwan National Science Council grant NSC 97-2320-B-010-027-MY3 (for IHC), NSC 98-2311-B-009-001-MY2 (for EH), and a grant from Taiwan Ministry of Education, Aim for the Top University Plan.

REFERENCES

Adriaenssens T, Mazoyer C, Segers I, Wathlet S, Smitz J (2009) Differences in collagen expression in cumulus cells after exposure to highly purified menotropin or recombinant follicle-stimulating hormone in a mouse follicle culture model. Biol Reprod 80:1015–1025.

Brazil D, Park J, Hemmings B (2002) PKB binding proteins: getting in on the Akt. Cell 111:293–303.

Brunet A, Datta SR, Greenberg ME (2001) Transcription-dependent and -independent control of neuronal survival by the PI3K-Akt signaling pathway. Curr Opin Neurobiol 11:297–305.

Bruns RR, Press W, Engvall E, Timpl R, Gross J (1986) Type VI collagen in extracellular, 100-nm periodic filaments and fibrils: identification by immunoelectron microscopy. J Cell Biol 103: 393–404.

Burke RE (2007) Inhibition of mitogen-activated protein kinase and stimulation of Akt kinase signaling pathways: two approaches with therapeutic potential in the treatment of neurodegenerative disease. Pharmacol Ther 114:261–277.

Caridad R, Karin M (1996) Ultraviolet light and osmotic stress: activation of the JNK cascade through multiple growth factor and cytokine receptors. Science 274:1194–1197.

Cheng JS, Dubal DB, Kim DH, Legleiter J, Cheng IH, Yu G-Q, Tesseur I, Wyss-Coray T, Bonaldo P, Mucke L (2009) Collagen VI protects neurons against Aβ toxicity. Nat Neurosci 12:119–121.

Cheresh DA, Stupack DG (2008) Regulation of angiogenesis: apoptotic cues from the ECM. Oncogene 27:6285–6298.

Chu Y-F, Brown PH, Lyle BJ, Chen Y, Black RM, Williams CE, Lin Y-C, Hsu C-W, Cheng IH (2009) Roasted coffees high in lipophilic antioxidants and chlorogenic acid lactones are more neuroprotective than green coffees. J Agric Food Chem 57:9801–9808.

Datta SR, Brunet A, Greenberg ME (1999) Cellular survival: a play in three Akts. Genes Dev 13:2905–2927.

Datta SR, Dudek H, Tao X, Masters S, Fu H, Gotoh Y, Greenberg ME (1997) Akt phosphorylation of BAD couples survival signals to the cell-intrinsic death Machinery. Cell 91:231–241.

Daub A, Sharma P, Finkbeiner S (2009) High-content screening of primary neurons: ready for prime time. Curr Opin Neurobiol 19: 537–543.

Davis RJ (2000) Signal transduction by the JNK group of MAP kinases. Cell 103:239–252.

Dérijard B, Hibi M, Wu I-H, Barrett T, Su B, Deng T, Karin M, Davis RJ (1994) JNK1: a protein kinase stimulated by UV light and Ha-Ras that binds and phosphorylates the c-Jun activation domain. Cell 76:1025–1037.

Dhanasekaran DN, Reddy EP (2008) JNK signaling in apoptosis. Oncogene 27:6245–6251.

Dityatev A, Fellin T (2008) Extracellular matrix in plasticity and epileptogenesis. Neuron Glia Biol 4:235–247.

Dityatev A, Schachner M (2003) Extracellular matrix molecules and synaptic plasticity. Nat Rev Neurosci 4:456–468.

Fitzgerald J, Rich C, Zhou FH, Hansen U (2008) Three novel collagen vi chains, α4(VI), α5(VI), and α 6(VI). J Biol Chem 283:20170–20180.

Fox MA (2008) Novel roles for collagens in wiring the vertebrate nervous system. Curr Opin Cell Biol 20:508–513.

Hatamochi A, Aumailley M, Mauch C, Chu ML, Timpl R, Krieg T (1989) Regulation of collagen VI expression in fibroblasts. Effects of cell density, cell-matrix interactions, and chemical transformation. J Biol Chem 264:3494–3499.

Howell SJ, Doane KJ (1998) Type VI collagen increases cell survival and prevents anti-beta1 integrin-mediated apoptosis. Exp Cell Res 241:230–241.

Hubert T, Grimal S, Carroll P, Fichard-Carroll A (2009) Collagens in the developing and diseased nervous system. Cell Mol Life Sci 66:1223–1238.

Irwin WA, Bergamin N, Sabatelli P, Reggiani C, Megighian A, Merlini L, Braghetta P, Columbaro M, Volpin D, Bressan GM, Bernardi P, Bonaldo P (2003) Mitochondrial dysfunction and apoptosis in myopathic mice with collagen VI deficiency. Nat Genet 35:367–371.

Iyengar P, Espina V, Williams TW, Lin Y, Berry D, Jelicks LA, Lee H, Temple K, Graves R, Pollard J, Chopra N, Russell RG, Sasisekharan R, Trock BJ, Lippman M, Calvert V, Petricoin F, Liotta L, Dadachova E, Pestell RG, Lisanti MP, Bonaldo P, Scherer PE (2005) Adipocyte-derived collagen VI affects early mammary tumor progression *in vivo*, demonstrating a critical interaction in the tumor/stroma microenvironment. J Clin Invest 115:1163–1176.

Kanazawa I (2001) How do neurons die in neurodegenerative diseases? Trends Mol Med 7:339–344.

Khan T, Muise ES, Iyengar P, Wang ZV, Chandalia M, Abate N, Zhang BB, Bonaldo P, Chua S, Scherer PE (2009) Metabolic dysregulation and adipose tissue fibrosis: role of collagen VI. Mol Cell Biol 29:1575–1591.

Khwaja A, Rodriguez-Viciana P, Wennstrom S, Warne PH, Downward J (1997) Matrix adhesion and Ras transformation both activate a phosphoinositide 3-OH kinase and protein kinase B/Akt cellular survival pathway. EMBO J 16:2783–2793.

Kielty CM, Whittaker SP, Grant ME, Shuttleworth CA (1992) Type VI collagen microfibrils: evidence for a structural association with hyaluronan. J Cell Biol 118:979–990.

Kim MA, Kim HJ, Jee HJ, Kim AJ, Bae YS, Bae SS, Yun J (2009) Akt2, but not Akt1, is required for cell survival by inhibiting activation of JNK and p38 after UV irradiation. Oncogene 28:1241–1247.

Kuo H-J, Maslen CL, Keene DR, Glanville RW (1997) Type VI collagen anchors endothelial basement membranes by interacting with type IV collagen. J Biol Chem 272:26522–26529.

Lampe AK, Bushby KMD (2005) Collagen VI related muscle disorders. J Med Genet 42:673–685.

Lampe AK, Zou Y, Sudano D, Brien KKO, Hicks D, Laval SH, Charlton R, Jimenez-Mallebrera C, Zhang RZ, Finkel RS, Tennekoon G, Schreiber G, Knaap MS, Marks H, Straub V, Flanigan KM, Chu ML, Muntoni F, Bushby KMD, Bönemann CG (2008) Exon skipping mutations in collagen VI are common and are predictive for severity and inheritance. Hum Mutat 29:809–822.

Lee TW, Tsang VWK, Birch NP (2008) Synaptic plasticity-associated proteases and protease inhibitors in the brain linked to the processing of extracellular matrix and cell adhesion molecules. Neuron Glia Biol 4:223–234.

Lu X, Lane DP (1993) Differential induction of transcriptionally active p53 following UV or ionizing radiation: defects in chromosome instability syndromes. Cell 75:765–778.

Meijering E, Jacob M, Sarria JCF, Steiner P, Hirling H, Unser M (2004) Design and validation of a tool for neurite tracing and analysis in fluorescence microscopy images. Cytometry A 58A:167–176.

Milner R, Campbell IL (2002) The integrin family of cell adhesion molecules has multiple functions within the CNS. J Neurosci Res 69:286–291.

Narro ML, Yang F, Kraft R, Wenk C, Efrat A, Restifo LL (2007) NeuronMetrics: software for semi-automated processing of cultured neuron images. Brain Res 1138:57–75.

Nelson CM, Bissell MJ (2006) Extracellular matrix, scaffolds, and signaling: tissue architecture regulates development, homeostasis, and cancer. Annu Rev Cell Dev Biol 22:287–309.

Palma E, Tiepolo T, Angelin A, Sabatelli P, Maraldi NM, Basso E, Forte MA, Bernardi P, Bonaldo P (2009) Genetic ablation of cyclophilin D rescues mitochondrial defects and prevents muscle apoptosis in collagen VI myopathic mice. Hum Mol Genet 18:2024–2031.

Parcellier A, Tintignac LA, Zhuravleva E, Hemmings BA (2008) PKB and the mitochondria: AKTing on apoptosis. Cell Signal 20:21–30.

Rosette C, Karin M (1996) Ultraviolet light and osmotic stress: activation of the JNK cascade through multiple growth factor and cytokine receptors. Science 274:1194–1197.

Ruehl M, Wiecher D, Sahin E, Somasundaram R, Riecken E-O, Schuppan D (1999) Soluble collagen VI as an auto/paracrine inhibitor of apoptosis in hepatic stellate cells. Gastroenterology 116:L0392.

Ruhl M, Sahin E, Johannsen M, Somasundaram R, Manski D, Riecken EO, Schuppan D (1999) Soluble collagen VI drives serum-starved fibroblasts through S phase and prevents apoptosis via down-regulation of Bax. J Biol Chem 274:34361–34368.

Schreier T, Winterhalter KH, Trüb B (1987) The tissue form of chicken type VI collagen. FEBS Lett 213:319–323.

Sherman-Baust CA, Weeraratna AT, Rangel LBA, Pizer ES, Cho KR, Schwartz DR, Shock T, Morin PJ (2003) Remodeling of the extracellular matrix through overexpression of collagen VI contributes to cisplatin resistance in ovarian cancer cells. Cancer Cell 3:377–386.

Sunayama J, Tsuruta F, Masuyama N, Gotoh Y (2005) JNK antagonizes Akt-mediated survival signals by phosphorylating 14-3-3. J Cell Biol 170:295–304.

Telfer WR, Busta AS, Bonnemann CG, Feldman EL, Dowling JJ (2010) Zebrafish models of collagen VI-related myopathies. Hum Mol Genet 19:2433–2444.

Washbourne P, Dityatev A, Scheiffele P, Biederer T, Weiner JA, Christopherson KS, El-Husseini A (2004) Cell adhesion molecules in synapse formation. J Neurosci 24:9244–9249.

Zhang J, Wang Q, Zhu N, Yu M, Shen B, Xiang J, Lin A (2008) Cyclic AMP inhibits JNK activation by CREB-mediated induction of c-FLIPL and MKP-1, thereby antagonizing UV-induced apoptosis. Cell Death Differ 15:1654–1662.

Zhang Y, Zhou X, Degterev A, Lipinski M, Adjeroh D, Yuan J, Wong STC (2007) Automated neurite extraction using dynamic programming for high-throughput screening of neuron-based assays. Neuroimage 35:1502–1515.

(Accepted 25 March 2011)
(Available online 1 April 2011)